Elevated Temperature Performance of Concrete Beams Reinforced with FRP Bars

ADVANCED
COMPOSITES IN
CONSTRUCTION 2015

Elevated Temperature Performance of Concrete Beams Reinforced with FRP Bars

Emma R.E. McIntyre, Luke A. Bisby, Tim J. Stratford
BRE Centre for Fire Safety Engineering
Institute for Infrastructure and Environment
The King's Buildings
The University of Edinburgh
EH9 3JL, UK

ABSTRACT

A key consideration in the application of FRP reinforcement in concrete is the mechanical and bond performance at elevated temperature. Tensile tests on FRP bars previously carried out at the University of Edinburgh have demonstrated that, whilst significant reductions in ultimate tensile strength were observed after the onset of decomposition of the polymer resin, FRPs' absolute tensile strength remained higher in comparison with steel reinforcing bars. It may therefore be reasonable to assume that the 'critical temperature' for FRP bars is above their glass transition temperature (T_g), provided that 'cold' anchorage zones can be assured. Thirty-two reinforced concrete (RC) beams were tested with either continuous or lap spliced FRP or steel reinforcement; tests were performed both at ambient temperature and under sustained load with transient localised heating. Glass and carbon FRP bars were both studied, as was conventional steel reinforcement. Cold anchorage of the reinforcement was maintained throughout testing. Minimum concrete cover ensured that FRP bar temperatures exceeded T_g during 90 minutes of heating. The results demonstrate that cold anchorage (i.e. maintained below T_g) of FRP bars is necessary to ensure their safe use as internal reinforcement in concrete, unless unrealistically deep concrete cover is provided. Where cold anchorage is provided, the performance of FRP bars is demonstrated – for the particular conditions of the current study – to be satisfactory under full service loads and at reinforcement temperatures exceeding 500°C.

INTRODUCTION

In conventional steel-reinforced concrete structures, the critical temperature of the reinforcing bars, when exposed to fire, is typically defined by a 50% reduction in yield strength of the reinforcement [1, 2]. If critical temperatures for FRP reinforcing bars are defined on this basis, as has been previously suggested in the literature [2], their critical temperatures will be much lower than for steel, due to complex softening and pyrolysis of the polymer resins used in their manufacture, at comparatively low temperatures. The mechanical properties of FRP bars degrade at temperatures close to their glass transition temperature (T_g) [1, 2]. In particular, the bond between FRP bars and concrete is almost completely lost at temperatures above T_g. However, despite bond strength reductions at temperatures near T_g, the fibres retain considerable tensile strength at much higher temperatures. Thus, for FRPs to be effective in fire, a strong FRP-concrete bond must be maintained; for straight bars this requires maintenance of a "cool" anchorage zone. This paper presents the use of cool anchorage as a means of ensuring fire resistance for FRP RC beams, and focuses on determining the critical temperatures both to maintain anchorage and to cause reinforcement rupture due to loss of tensile capacity.

EXPERIMENTAL PROGRAM

Three commercially available FRP bars have been used in the current study; two glass FRPs and one carbon FRP. These are denoted as BPG, PTG and PTC, and are shown in Figure 1. Bar BPG has a nominal 10 mm diameter with a double helical wrap and a fine sand coating as its surface treatment, whereas bars PTG and PTC have 9.5 mm nominal diameters and a coarse sand surface treatment. Conventional 10 mm diameter deformed steel bars were also studied for comparison.

Manufacturer-specified characteristics of all three FRP bars are given in Table 1. The T_g values for the respective bars were determined by dynamic mechanical analysis (DMA) and differential scanning calorimetry (DSC), and by applying various accepted T_g definitions under each test method [3]. Table 2 shows the considerable variation in T_g values obtained from various test methods and specific definitions.

Figure 1. (a) BPG (b) PTG, and (c) PTC Reinforcing Bars

Table 1. FRP Manufacturer Specified Properties

	BPG	**PTG**	**PTC**
Bar #	3	3	3
Nominal Diameter (mm)	10	9.5	9.5
Fibre Type	Glass	Glass	Carbon
Fibre Content (% Weight)	83.6	83	Not Specified
Resin	Vinyl Ester	Modified Vinyl Ester	Modified Vinyl Ester
Min. Tensile Strength (MPa)	1126	889	1431
Modulus of Elasticity (GPa)	63.2	53.4	120
Tensile Strain at Failure (%)	2.07	1.66	1.33

Table 2. FRP Glass Transition Temperatures Determined by the Authors' Testing

	Glass Transition Temperature, T_g (°C)			
	T_g[a]	T_g[b]	T_g[c]	T_g[d]
BPG	86	109	136	149
PTG	83	107	153	156
PTC	64	86	108	157

[a] defined by onset of loss of storage modulus in DMA testing
[b] defined by peak rate of loss of storage modulus in DMA testing
[c] defined by peak phase change between elastic and viscoelastic response (Tan δ Peak) in DMA testing
[d] defined by first notable thermal reaction in DSC testing

Concrete beams with a length of 1450 mm and a 150 mm square cross section, with a single tensile reinforcing bar, were designed in accordance with ACI 440.1 [4]. These were cast with steel or FRP reinforcement in either continuous or midspan-spliced arrangements, with a midspan bar splice length of 420 mm (see Figure 2).

Steel shear reinforcement (6mm diameter) was included outside the constant moment region; with the beams tested in 4-point bending as shown in Figures 2 and 3.The concrete had a 28-day cylinder strength of 34MPa (with a standard deviation of 1.38MPa). In the beams reinforced with continuous FRP bars a single strain gauge was placed on the tensile reinforcing bar at midspan, while 3 strain gauges were placed evenly along the midspan in the spliced FRP reinforced beams. Linear potentiometers were used to measure displacements and bar slip (Figure 3). A thermocouple (TC) tree with 5 TCs was embedded in the concrete at the centre of the each beam, allowing temperature measurements to be taken at depths of 0, 20, 30, 75 and 120 mm from the heated soffit (Figure 3). Two additional TCs were installed, either at one end of the constant moment region (continuous reinforcement) or at one end of the splice zone, at both 0 and 20 mm from the soffit. Image correlation was also used for strain and displacement measurement.

Beams were tested in duplicate at ambient temperature or under sustained loads, with transient localised heating of the constant moment region. Beams at ambient were tested at 2 mm/min until

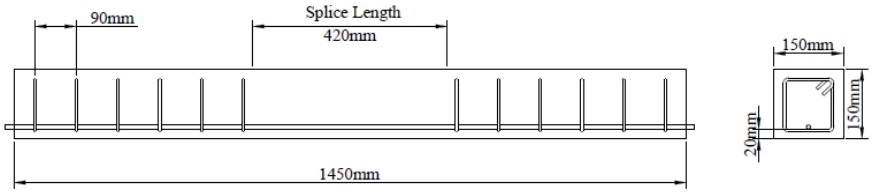

Figure 2. Reinforcement Detailing

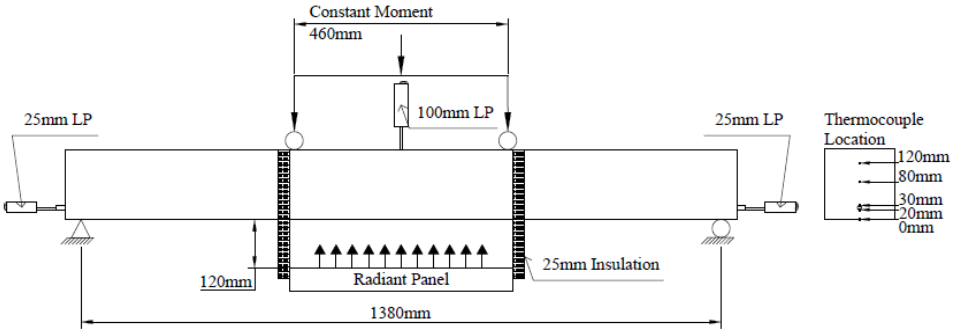

Figure 3. Test Setup

failure, whereas transient heated tests were loaded to sustained service loads and then heated from below with a propane-fired radiant panel until failure, or for 90 minutes if no failure occurred. For steel reinforced beams, load level was chosen based on 50% of ultimate capacity. Loads in excess of the GFRP creep rupture limit (ACI 440.1) were used for GFRP reinforced beams, and also CFRP beams as a comparison). The heated area was controlled using insulation boards to ensure cold anchorage for the flexural reinforcement outside the heated zone (Figure 3). If no failure occurred during heating the beam was left to cool for 60 minutes under sustained load before the load was released, and the beam was allowed to cool to room temperature before residual testing at a minimum of 2 weeks after heating.

RESULTS AND DISCUSSION

Summarised test data for the ambient and heated tests are shown in Tables 3 and 4 respectively, along with beam designations based on test variables. Figures 4 and 5 show load deflection responses for ambient and heated tests, respectively. SA-denoted beams, continuous and spliced, experienced classical under-reinforced flexural failures at large deformations. Spliced beams displayed a stiffening effect due to the presence of additional reinforcement in the midspan region. Both PTGA and BPGA spliced beams failed within the splice region, coincident with concrete cover separation. Continuous PTGA and BPGA beams failed due to tensile rupture of the bars at the location of flexural shear crack, along with localised concrete crushing. PTC beams failed due to a bond failure inside the anchorage zones, wherein the CFRP bars' surface coating governed the behaviour and the bars slipped inside the beams. The strains in the respective reinforcing bars at peak loads are given in Table 3, and indicate the utilization of the various types of reinforcement at peak load (refer back to Table 1). Figure 5 shows the central deflections of the beams during the heated tests, through 90 minutes of heating and 60 minutes of cooling. Some beams are not shown due to malfunctioning of the deflection gauges during heating. Time zero is the onset of heating, after beams had been loaded (see Table 4). In all cases there is an increase in deflection during initial heating. This is due to thermal bowing of the beams resulting from the thermal gradients that are generated upon heating. This is followed by steady deflection increases, with differing responses depending on the reinforcement type and whether the reinforcement is continuous or spliced.

Detailed discussions of the heating and cooling responses are not possible in the current paper. However, SH beams displayed steady deflection during heating with decreases in deflection during cooling, as expected. PTCHc beams showed similar behavior, however deflections continued to increase, albeit at a lower rate, during cooling; BPGHc beams failed by bar rupture when the bar exceeded temperatures in the range 349-531°C; PTGHc beams survived the 90 minutes of heating, despite the bars experiencing temperatures in the range 423-526°C and the beams displaying very large deflections. For the GFRP continuous beams, there is an increase in central displacement between 45-60 minutes into the heating cycle. Interestingly, this coincides with the decomposition of the FRP matrix, as determined by TGA tests. The peak mass loss of the FRP samples approximately occurred at 390°C and 420°C for PTG and BPG GFRP bars, respectively.

Table 3. Ambient Beam Test Results

Name	Fibre Type	Bar Continuity	Peak Capacity (kN)	Approx. Strain in Bars at Peak Capacity (%)	Central Disp. at Peak Capacity (mm)
SAc1	Steel	Continuous	22.4	-	46.0
SAc2	Steel	Continuous	22.9	-	63.0
SAs1	Steel	Spliced	24.4	-	22.2
SAs2	Steel	Spliced	26.2	-	39.9
BPGAc1	Glass	Continuous	34.8	1.43	45.6
BPGAc2	Glass	Continuous	35.5	1.27	30.3
BPGAs1	Glass	Spliced	36.7	1.28	25.5
BPGAs2	Glass	Spliced	35.9	1.32	26.4
PTGAc1	Glass	Continuous	30.6	1.06	39.0
PTGAc2	Glass	Continuous	34.2	Failed Gauge	41.3
PTGAs1	Glass	Spliced	27.4	1.42	24.6
PTGAs2	Glass	Spliced	27.8	1.29	24.0
PTCAc1	Carbon	Continuous	39.8	0.81	21.7
PTCAc2	Carbon	Continuous	37.4	>0.67[1]	21.0
PTCAs1	Carbon	Spliced	36.3	0.67	15.7
PTCAs2	Carbon	Spliced	37.2	0.62	17.6

[1]Indicates last recorded value as strain gauge failed 1 minute prior to failure of the beam

Table 4. Heating Beam Test Results

Name	Fibre Type	Bar Continuity	Sustained Load (kN)	Bar Strain at Ignition[2] (%)	Time to Failure (min)	Peak Bar Temp.[3] (˚C)	Residual Capacity (kN)
SHc1	Steel	Continuous	10.7	-	-	499[4]	25.0
SHc2	Steel	Continuous	10.9	-	-	475	25.0
SHs1	Steel	Spliced	10.9	-	-	474	21.7
SHs2	Steel	Spliced	10.8	-	-	498	17.6
BPGHc1	Glass	Continuous	13.3	27.2	63	499	-
BPGHc2	Glass	Continuous	13.1	26.8	82	531	-
BPGHs1	Glass	Spliced	13.0	26.7	11	181	-
BPGHs2	Glass	Spliced	13.1	26.8	11	167	-
PTGHc1	Glass	Continuous	10.6	31.7	-	566	10.7
PTGHc2	Glass	Continuous	10.6	31.4	-	526	15.7
PTGHs1	Glass	Spliced	10.6	31.8	16	260	-
PTGHs2	Glass	Spliced	10.6	31.8	17	249	-
PTCHc1	Carbon	Continuous	17.6	30.2	-	556	34.1
PTCHc2	Carbon	Continuous	17.6	30.0	-	560	30.7
PTCHs1	Carbon	Spliced	17.6	29.9	7	57[4]	-
PTCHs2	Carbon	Spliced	17.6	30.0	7	104	-

[2] as a percentage of the manufacturers' specified ultimate tensile strain (calculated from a plane section analysis under specified service load)

[3] Temperatures recorded from the lower surface of the bar at midspan
[4] Measurement taken from upper surface of the reinforcing bar

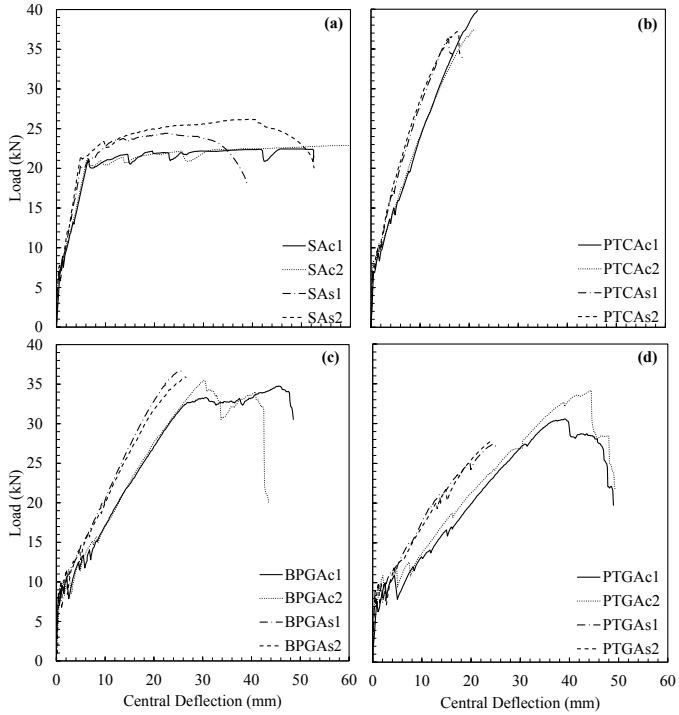

Figure 4. Ambient Temperature Load-Deflection Responses for: (a) Steel, (b) PTC, (c) BPG, and (d) PTG reinforced beams

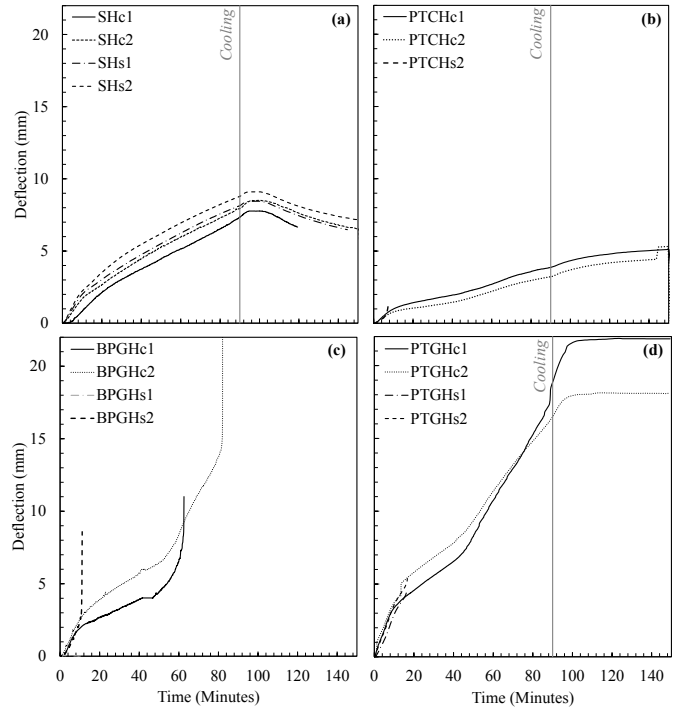

Figure 5. Heated Beam Deflection from the Onset of Heating for: (a) Steel, (b) PTC, (c) BPG, and (d) PTG reinforced beams

All spliced FRP reinforced beams failed early during heating due to splice failure in the midspan region, with temperatures at the level of the reinforcement in the splice in the range of T_g; somewhat above T_g in the case of PTG bars. This may indicate a difference in the response of carbon FRPs versus glass FRPs. In table 4, the residual capacity of the beams is shown. The CFRP beams showed more than 80% retention of residual capacity despite the CFRP fibres in the heated zone experiencing temperatures in the range 438-560°C. In comparison the GFRP reinforced beams, retained only 40% of their ambient capacity after heating despite experiencing similar temperatures. This may be due to degradation of the glass fibres as temperatures exceed 500°C.

CONCLUSIONS

The tests have confirmed that cold anchorage for FRP reinforced beams is essential to ensure that failure does not occur due to loss of bond by their exposure to temperatures exceeding their respective T_g values. The spliced beam tests demonstrated that failure was likely when the T_g range had been exceeded at the level of the FRP reinforcement. Temperatures somewhat higher than T_g were needed to cause failure for the PTG GFRP reinforced beams, likely due to the sustained strain in the FRP during heating being sufficiently low (30% of ultimate) allowing anchorage to be maintained for a short duration above T_g. The results further indicate that thermal degradation of an FRP's fibres themselves may affect both fire endurance and residual capacity.

The following preliminary recommendations, for the specific FRP bars tested herein, can be made:

1) If cool anchorage of the tensile reinforcement cannot be provided, the limiting temperature should be conservatively taken as the lowest of the measured T_g values.
2) Until more data is available, 'cool anchorage' should be defined as a length of reinforcement that can develop full ambient temperature capacity; this must be maintained below the limiting temperature noted in (1) above.
3) Where cool anchorage can be provided, and sustained tensile strain in glass and carbon FRP is less than 30% of ultimate at the onset of heating, the experiments suggest critical temperature for FRP bars may be defined based on reductions of tensile properties of the fibres, rather than the polymer matrix. Conservatively however, a limiting temperature should be based on the onset of decomposition of the polymer matrix, $T_{d,onset}$, which would be preferable when considering residual capacity. It is hypothesised that this may be applicable to all FRP bars but additional research is needed before this concept should be applied in design.
4) Surface treatment and secondary curing of the coating on FRP bars should be carefully considered both during manufacture and for the purposes of design, since the longitudinal shear stress transfer capacity of the bars' coating may impede FRP reinforcement being used to full effect, particularly for CFRP bars.

ACKNOWLEDGEMENTS

The authors gratefully acknowledge the support of the UK Engineering Physical Sciences Research Council EPSRC and industry partners BP Composites and Pultrall Inc. Bisby gratefully acknowledges the support of Ove Arup and Partners and the Royal Academy of Engineering. The authors are members of the Edinburgh Research Partnership in Engineering (ERPE).

REFERENCES

1. McIntyre, E., Bilotta, A., Bisby, L., and Nigro, E., Mechanical Properties of Fibre Reinforced Polymer Reinforcement for Concrete at High Temperature presented at the *8th International Conference on Structures in Fire*, Shanghai, China, 11-13 June, 2014
2. Bisby, L., Kodur, V., Evaluating the fire endurance of concrete slabs reinforced with FRP Bars: Considerations for a holistic approach, Composites Part B, **38**, 547-558 (2007).
3. Bakis, C., Bisby, L., Lopez, M., Witt, S., Alkhrdaji, T, Interlaboratory evaluation of Tg of ambient-cured epoxies used in civil infrastructure presented at the *7th International Conference on FRP Composites in Civil Engineering*, Vancouver, Canada, 20-22 August 2014
4. ACI440.1R-06, Guide for the Design and Construction of Structural Concrete Reinforced with FRP Bars, American Concrete Institute, 2006